

Tilting Pad Journal Bearings— Measured and Predicted Stiffness Coefficients[©]

D. W. PARKINS (Member, STLE)
Cranfield Institute of Technology
Bedford, United Kingdom
and

D. HORNER
Michell Bearings
Newcastle-upon-Tyne, United Kingdom

This paper presents measured and calculated characteristics of a tilting pad journal bearing suitable for high speed machinery. Descriptions are given of the experimental techniques used with this variety of bearing and the theoretical model for predicting performance.

Measured values of pad temperature, eccentricity, attitude angle, and the four stiffness coefficients are given for a range of loads and rotational speeds. Data are given for both load on pad and between pad configurations, the two principal loading arrangements.

Comparisons are made between the measured and predicted bearing temperatures and stiffness coefficients over a wide range of values.

KEYWORDS

Bearings, Hydrodynamic, Tilting Pad, Load Carrying Capacity

INTRODUCTION

Tilting pad journal bearings have been used to support rotating shafts for a considerable number of years. They are more expensive and occupy a larger space than a cor-

responding conventional plain bearing. Nonetheless, they have been, and continue to be, selected by designers in applications where their superior stability, especially in the high speed/low load condition, is a paramount consideration.

Consequently, as with plain bearings, their widespread use has preceded knowledge of their performance characteristics and reliable theoretical models thereof. It is only in relatively recent times that the performance of tilting pad journal bearings has been studied. Theoretical studies (1)–(3) have been reported, and in particular Jones and Martin (4) have indicated the effect of changes in various geometrical parameters upon performance. Within the last few years, results of a number of experimental studies (5)–(9) have been published. Notwithstanding, there remains a scarcity of data.

This paper presents a contribution to this knowledge by comparing the measured performance of a typical tilting pad journal bearing with the predicted characteristics. Data are given for both the common operating configurations of load on and load between pads.

BEARING AND TEST DETAILS

The basic details of the tilting pad bearing selected for the test program are outlined in Table 1. The bearing was a standard 80 mm unit with a length to diameter ratio of 0.4 and a proprietary design as illustrated in Fig. 1. These units consisted of five tilting pads retained in a split-bearing housing, with end baffles to control the oil discharge. The

Presented as a Society of Tribologists and Lubrication Engineers paper at the ASME/STLE Tribology Conference in San Diego, California, October 19–21, 1992
Final manuscript approved June 29, 1992

NOMENCLATURE

a_{yy}, a_{xx} = oil film stiffness coefficients
 a_{yx}, a_{xy} =
 C_a = bearing assembled clearance, difference between journal radius and the distance from bearing center to pad surface, as installed
 C_p = pad surface clearance, difference between pad face machined surface and journal radius
 D = journal diameter
 L = bearing length
 N = rotational speed
 P_h, P_v = forces applied to the bearing housing, horizontal and vertical

T = temperature
 W = steady load
 h, v = coordinates of journal center, horizontal and vertical
 x, y = coordinates of journal center, perpendicular and parallel to the load direction
 α = steady load direction (Fig. 3a)
 ϵ = journal eccentricity
 ϕ = attitude angle
 Δ_1, Δ_2 = journal center displacements from equilibrium position due to the application of incremental loads ΔP_h and ΔP_v
 η = viscosity of the lubricating fluid

TABLE 1—BEARING AND TEST DETAILS	
Bearing geometry	
Journal diameter	80 mm (3.149 inch)
Journal length	32 mm (1.260 inch)
Clearances (radial)	
C_a (assembled)	0.047 mm (0.00185 inch)
C_p (pad surface)	0.104 mm (0.00409 inch)
Pad preload ratio	0.55 ($C_p - C_a$)/ C_p
Number of pads	5
Circumferential arc	60 degrees
Lubrication	
Oil type	Shell Turbo 32
supply temperature	45–50°C
supply pressure	27–48 kPa (4.0–7.0 lbf/in ²)
Bearing duty	
Load	0.5 – 5.0 kN (112–1124 lbf)
Rotational speed	3000–8800 rpm

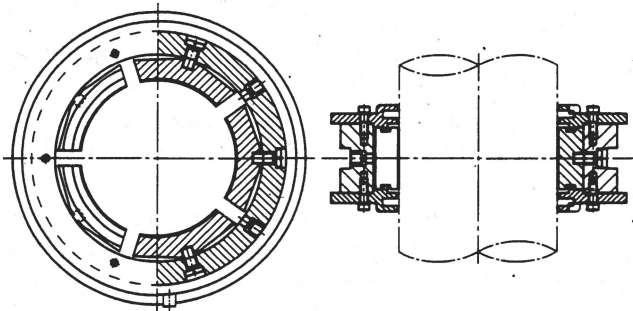


Fig. 1—Test bearing assembly.

bearing normally operated with the housing filled with oil.

The tilting pads were held in the bearing housing so that they were preloaded towards the journal, and the five radial oil feed holes were located at the inter pad spaces. The pads themselves were of the central line pivot type, with a 0.5 mm thick white-metal (babbitt) face on a steel backing 12 mm thick. Apart from a break for the pad locating stop, the pivot extended the full width of the pad. This resulted in a pivot strength of more than $2.0E+9 \text{ Nm}^{-1}$, which is an order of magnitude greater than the expected lubricating film stiffnesses.

The lubricant used in this series of tests was an ISO 32 grade turbine oil (32cSt at 40°C and 21cSt at 50°C). Throughout all the tests reported herein, the temperature of the oil at inlet to the bearing assembly was maintained in the range 45° to 50°C. Typically the temperature variation during the course of a test sequence was less than 3°C.

Tests were performed at loads of 0.5, 1.0, 3.0, and 5.0 kN, which cover the typical working range of 0.2 to 2.0 MPa (30 to 300 psi) mean bearing pressure. The shaft speeds used for the test program were 3000, 5000, and 8800 rpm, this range being limited by the capabilities of the test stand.

Non-contacting displacement transducers mounted on the bearing housing measured the relative journal center position in the horizontal and vertical directions (h, v) at axial stations on either side of the bearing. The lowest pad was fitted with a chromel-alumel thermocouple adjacent to the

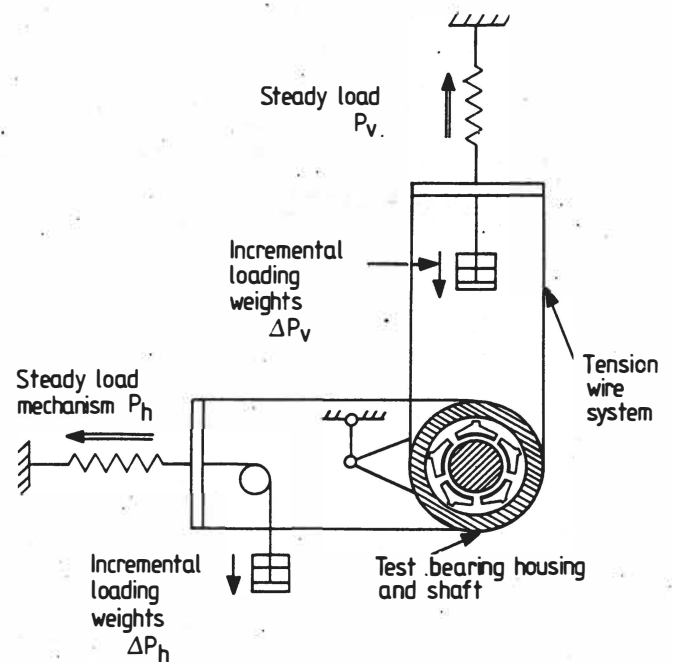


Fig. 2—Test equipment loading arrangement.

pad pivot to give an indication of mean oil temperature in the lubricating films. Inlet and outlet bulk oil temperatures were also recorded.

EXPERIMENTAL TECHNIQUE

An outline arrangement of the test stand illustrating its use in the work reported herein is shown in Fig. 2. A full description of the experimental apparatus and the arrangements for loading the test bearing having been published previously (10), (11).

The test bearing was suspended on the shaft between two rolling element support bearings. Loads were applied to the test bearing through tensioned wires in both the horizontal and vertical directions (h, v). By using an appropriate combination of forces P_h, P_v the steady load W could be applied at any angle α in a segment of 90° from vertical to horizontal ($0^\circ \leq \alpha \leq 90^\circ$). This provided a convenient means of directing the load either between pads 1 and 2 ($\alpha = 36^\circ$), directly at pad 1 ($\alpha = 0^\circ$), or directly at pad 2 ($\alpha = 72^\circ$), see Fig. 3a, without re-establishing thermal equilibrium and/or changing speed.

Use of the test stand to measure the assembled bearing's clearance space in the cold, non-rotating state, has been described in (10). The reference explains how a near complete clearance circle can be obtained for plain bushes by forcing the journal against the bearing surface at a large number of radial locations. However, the current test bearing's inherent pad tilting property meant that consistent readings could be obtained only when the journal was forced in the direction of an interpad gap. At all points in between, the journal slid along the tilted pad surface until it reached one of the interpad positions. Hence, only five consistent data points were reliably obtained.

Location of the effective bearing center in the hot rotating condition was accomplished using a new technique which

Tilting Pad Journal Bearings—Measured and Predicted Stiffness Coefficients

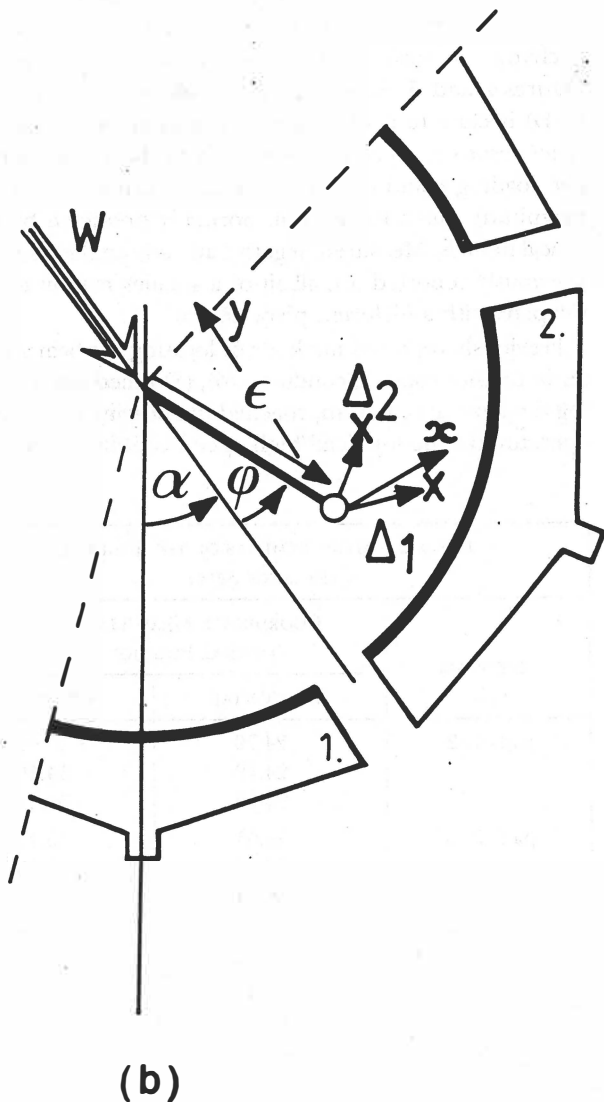
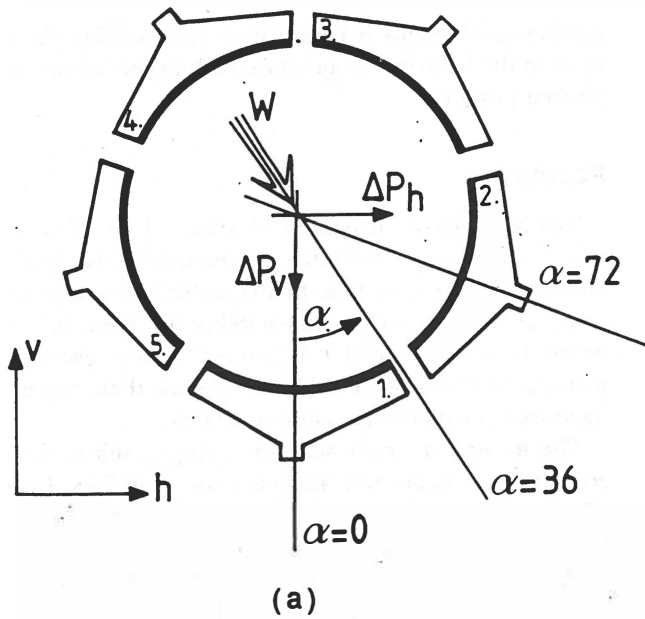


Fig. 3—Steady and incremental loading details.
 (a) Static and incremental loading
 (b) Bearing coordinates and displacements

was independent of the cold clearance space measurements. The new method utilized the ability of the test stand to direct the applied load to either of the pads at $\alpha = 0^\circ$ and 72° (nos. 1 and 2), and the symmetry of these loading conditions. The procedure assumes that the attitude angle and eccentricity remain the same for operation with the load directed towards each of the pads 1 and 2. Thus, successive measurements of the journal position, having achieved thermal equilibrium, at these two load directions, enabled the bearing center to be located in the transducer coordinates for that duty.

If the coordinates of the journal center are given for the loading directed at pads 1 and 2, respectively, by h_1, v_1 and h_2, v_2 then:

$$\epsilon = [(h_2 - h_1)^2 + (v_2 - v_1)^2]^{1/2} / 1.1756$$

Since the angle α could only be varied within the range $0 \leq \alpha \leq 90^\circ$ when the test rig was in the hot rotating condition, then the hot bearing center location procedure used only pads 1 and 2 for the given direction of rotation.

Having established the bearing center, a simple manipulation of the journal center coordinate measurements produced the eccentricity and attitude angle for the load on pad condition. Assuming this bearing center is valid for the load between pad operation ($\alpha = 36^\circ$), a further reading of the journal position gave the eccentricity and attitude angle for that case. This entire procedure formed the basis for determining the bearing's steady state operating condition for each and every load/speed combination.

The oil film stiffness coefficient $a_{xx} - a_{yy}$ were measured using a previously applied modification to the traditional incremental loading technique (10), (11). If, as in the traditional technique, incremental forces are applied in directions parallel and perpendicular to the loading direction, then difficulties arise in the measurement of the consequential incremental displacements when operating at high eccentricities. Problems arise because under such conditions, the four coefficients have very different magnitudes. For example, a typical set of stiffness coefficients $a_{xx}, a_{yy}, a_{yy}, a_{yx}$, for results quoted in this paper for eccentricity ratio 0.75 are respectively 105, -14, 105 and -14 MNm^{-1} (0.6, -0.08, 4.0, -0.08 10^{+6} lbf inch^{-1}). Separate application of typical incremental forces, (294 Newtons) (66.2 lbf) in directions parallel and perpendicular to the steady load, would give corresponding incremental displacements of $\Delta xa, \Delta xb, \Delta ya,$ and Δyb of +2.29, +0.055, +0.055, and 0.42 10^{-3} mm (110.0, 2.2, 2.2, 16.5 10^{-6} inch). These displacements have widely different magnitudes, in the extreme ratio of 50:1. Moreover, the values of 0.055 10^{-3} mm were judged to be less than the maximum possible error, not discrimination, of the measuring system when testing tilting pad bearings. Displacements between bearing and journal were measured in two planes on either side of the test bearing, from which values for the bearing center plane were computed. This meant that the maximum possible error for measurement in bearing center plane could take any value between zero and 0.127 10^{-3} mm (5.0 10^{-6} inch) depending on the sign of the error at each measuring station. A

smaller value was obtained with plain bearings. From this data it follows that the error in the magnitude of the derived value of the indirect coefficients a_{xy} , a_{yx} would be in the range zero to ± 120 percent with a reversal of sign. However, if the same typical incremental loads are applied in two separate directions other than parallel and perpendicular to the steady load, at say an angle $\alpha = 45^\circ$, then the corresponding displacements to be measured take nearly equal magnitudes and are well above the maximum possible error, i.e., 1.662, 1.187, 1.187, and $1.549 \cdot 10^{-3}$ mm (65.45, 46.73, 46.73 and $61.0 \cdot 10^{-6}$ inch). This reduces the range of possible error in derived cross coefficients to between zero and ± 30.7 percent, without a sign reversal. Previously reported applications of this approach (10), (11) describe testing of plain bearings with complete circumferential symmetry and utilize angles of 30° , 40° and 50° .

However, the tilting pad bearing does not have such circumferential symmetry. Indeed, symmetry only arises with the five pad variety under test at 72° intervals. Hence, in the tests reported herein, use of $\alpha = 72^\circ$ and 36° conveniently provided load on and between conditions with non-zero angle α . However, at these values of α , the accuracy benefit for the cross coefficients a_{xy} , a_{yx} for $\alpha = 36^\circ$ was less than that at 45° , namely, in the range zero to ± 45 percent instead of 30.7 percent and for $\alpha = 72^\circ$ only a slight improvement over the likely accuracy to be obtained at $\alpha = 0$. Accuracy of the determination of the direct coefficients a_{xx} , a_{yy} at $\alpha = 36^\circ$, 72° was less markedly affected by choice of angle α , being within the ranges zero to ± 14.5 to ± 30.3 percent (a_{yy}) and 0.4 to 1.7 percent (a_{xx}). This application of the procedure produced a useful reduction in scatter for most coefficients under most, but not all, conditions, while retaining the benefit of simplicity.

THEORETICAL MODEL

The predictions of the steady state operating condition and stiffness coefficients are calculated using a model previously described by Ettles (1). The computer program obtains a simultaneous set of solutions for oil film pressure, temperature, and pad distortion for each of the tilting pads in the bearing assembly.

The pressure in the lubricating fluid is generated by solving Reynolds equation using local oil film viscosities derived from the thermal analysis, with Constantinescu's allowance for non-laminar flow in the clearance space. The thermal analysis is based on viscous losses in the fluid with pre-heating of the lubricant at entry to the lubricating film and includes dissipation by convection along the film with conduction through the shaft and pads. The program also calculates distortion of the film shape by solving the elasticity and thermal expansion equations for the pads using the fluid temperature and pressure solutions.

The steady state performance is generated by solving the Reynolds, thermal, and elasticity equations at the required duty conditions. Because of the strong coupling between the film shape, temperature, and fluid pressure, a complex iterative procedure is used to balance all of the equations for each of the pads simultaneously. The calculation of the

stiffness coefficients is based upon recalculating the solutions to the basic set of equations with perturbations to the journal position.

RESULTS

The readings of the bearing clearance space taken in the cold non-rotating condition are presented in Table 2. The tabulated values show that the five stable interpad positions could be located with a repeatability of about 10^{-4} mm, which represents about 0.1 percent of the bearing diametrical clearance. As would be expected, these five in situ measured points lie very close to a circle.

The measured steady state operating positions, journal eccentricity, and attitude angle are shown in Figs. 4 and 5. The results were obtained from various combinations of load and speed within the range of duties 0.5 – 5.0 kN and 3000 – 8800 rpm. It is evident that the data points form groups of results at constant load but various speeds, indicating that load has the largest influence on operating eccentricity. In general, a threefold increase in speed has produced a 10 to 15 percent variation in eccentricity, while a change in load increased eccentricity by 30 percent. Figures 4 and 5 show that the steady state journal locus (ϵ , \emptyset) is close to a straight radial line, in conformity with other results (8). The data sets for both the on and between pad loading conditions show negative attitude angles of a magnitude much larger than normally predicted by theoretical models. Measured negative attitude angles have been previously reported (6), albeit of a smaller magnitude and for pads with a different pivot design.

Previously reported methods of locating the bearing center in the hot rotating condition (6), (8) relied upon assuming the journal center approached the bearing center when operating at the low load/high speed condition. Since the

TABLE 2—MEASUREMENTS OF THE JOURNAL CLEARANCE SPACE

INTERPAD GAP	COORDINATE MEASUREMENTS OF JOURNAL POSITION (μm)	
	HORIZONTAL	VERTICAL
pads 1-2	24.79	-54.05
	24.79	-54.10
	24.80	-54.23
pads 2-3	38.61	6.17
	38.63	6.15
	38.64	6.11
pads 3-4	-17.29	37.83
	-17.33	37.88
	-17.34	37.89
	-17.45	37.90
pads 4-5	-57.91	14.35
	-57.92	14.36
	-57.94	14.32
pads 5-1	-56.47	-53.51
	-56.44	-53.60
	-56.47	-53.57

LOAD ON PAD

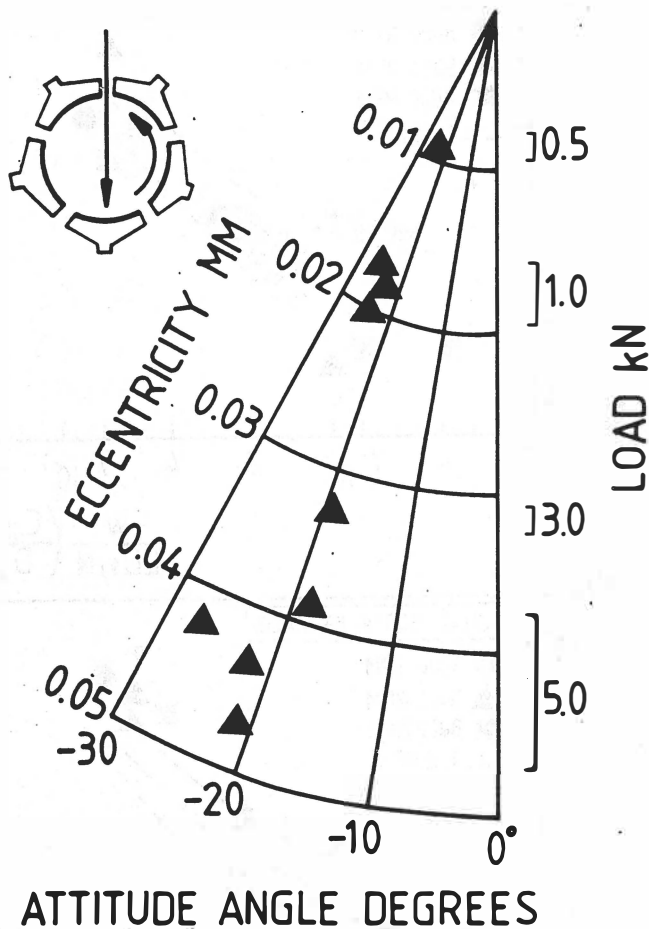


Fig. 4—Measured steady state journal locus, load on pad.

current work uses a different technique, as described in the previous sections, it is interesting to assess the location of the bearing center by applying the method of Tripp and Murphy (8) to the data reported in this paper. The results obtained from the two lowest load conditions, 0.5 kN and 1.0 kN, can be extrapolated both in magnitude and direction to find the predicted location of the bearing center. Evidently the result lies very close to the zero eccentricity point on the figure. Thus it is reasonable to deduce that the method of Tripp (8) and that reported herein are in close agreement on their bearing center location.

Figure 6 shows the measured and predicted pad temperature results for both the load on and between pad conditions. The values presented are the differences between the measured pad temperature at the specified location and the oil inlet temperature. As expected, the temperature difference increases with rotational speed, and to a lesser extent, load. Over the speed range studied, a change from a nominal load to the maximum rating produced a rise of 10°C in pad temperature, while a speed increase from 3000 to 8800 rpm produced an increase of 20°C. As would be expected, the difference between the load on and between pad conditions has only a small effect, with the load on pad condition producing the hotter temperatures. Inlet oil temperatures were maintained in the range 45° to 50°C for all cases shown in Fig. 6. At the highest rotational speed, the

LOAD BETWEEN PADS

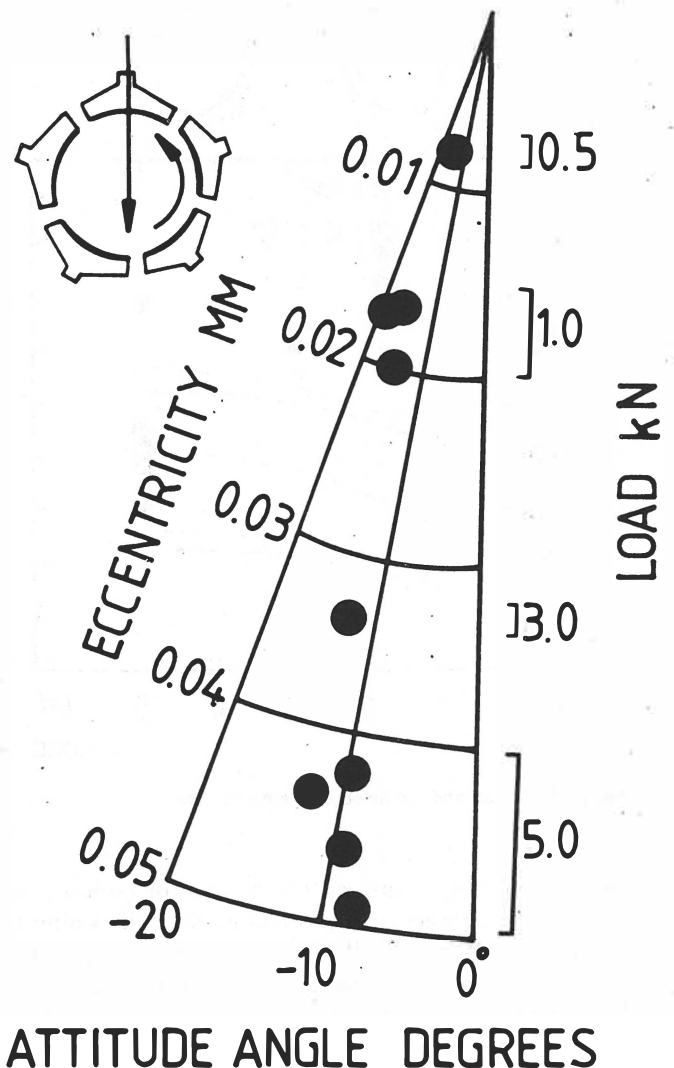


Fig. 5—Measured steady state journal locus, load between pads.

theoretical model underpredicts pad temperatures by about 3°C, otherwise theory correctly predicts all trends in proportion to their measured counterpart.

The results for the direct stiffness coefficients a_{yy} and a_{xx} are presented in Figs. 7 and 8, together with the predicted performance trends. These values are plotted against a horizontal scale of Sommerfeld number, which increases with increasing eccentricity ratio.

The figures show the expected trends of stiffness increasing with Sommerfeld number and the a_{yy} coefficient greater than the a_{xx} value at any given operating condition. These features are consistent with other findings (9). The magnitude of the stiffness coefficients reported herein are comparable with the values obtained by Brockwell and Dmochowski (9) for a bearing of similar journal diameter. However a detailed comparison is of limited value since their results have been obtained from a longer bearing operating at a much lower shaft speed, 1800 rpm, well below the typical working range for the size of bearing tested.

It is evident from the figures that the direct stiffness coefficients have similar values at the lowest Sommerfeld num-

Location of thermocouple in pad surface

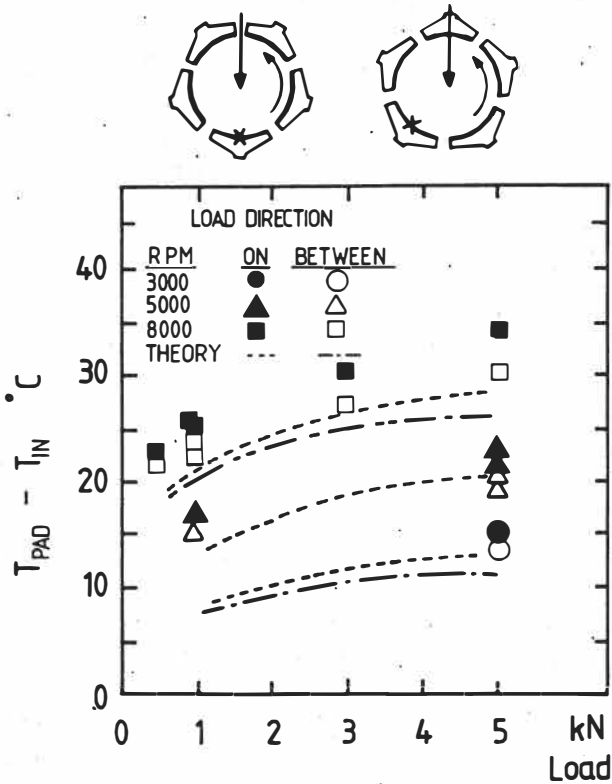


Fig. 6—Measured and predicted pad temperatures.

ber. Indeed, the a_{yy} and a_{xx} coefficients for both the load on pad and between pad configurations all lie within the relatively restricted range of 60 to 90 MNm^{-1} . This result is to be expected due to the symmetry of the central journal location in the five pad bearing geometry at low eccentricity ratios.

Traditionally tilting pad bearings have been assumed to operate at small attitude angles. Under these conditions, increasing the applied load with the load on pad case causes the journal to approach a pad directly, leading to a comparatively steep rise in the a_{yy} coefficient. For the load between pad case, a less marked rise in the a_{yy} stiffness is often expected since the journal more closely approaches an interpad space. However the lower pad temperature and the greater eccentricity observed for the load between pad condition have produced similar a_{yy} stiffness results for the two loading cases.

In contrast, the effect of loading condition on the a_{xx} coefficient is more pronounced. Figure 8 shows that the stiffness values for the on pad case are almost invariant with Sommerfeld number. This is because there is no significant change in the film thicknesses for the two pads producing the bulk of the journal's horizontal restraint, pads 2 and 5 show in Fig. 3a. For the load between pad case, the two pads carrying the applied load exert forces with strong horizontal components. Consequently the a_{xx} stiffness increases with the eccentricity ratio in the same manner as, but not as rapidly as, the a_{yy} coefficient. Hence, the independently produced stiffness characteristics are consistent and in reasonable agreement with predictions.

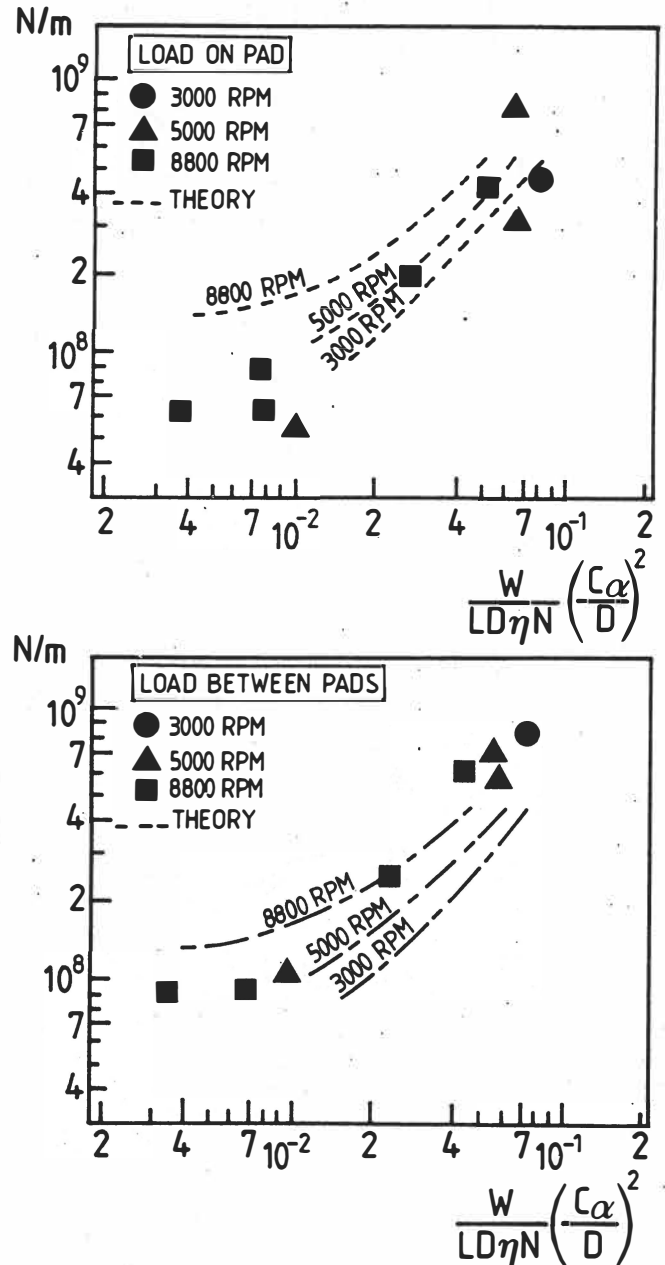


Fig. 7—Measured and predicted stiffness coefficient a_{yy} .

The measured cross-coupled stiffness coefficients a_{yx} and a_{xy} are shown in Fig. 9. The plot shows that for each of the two loading cases there is no appreciable difference between the two coefficients. For the load on pad case the stiffnesses are relatively small and not very significant. However, when the load is directed between pads, both coefficients formed a consistent set over the entire range of Sommerfeld numbers. These results should be considered significant since the cross-coupled stiffnesses attain values almost half that of the smaller direct coefficient a_{xx} . This is contrary to the usual expectation that the cross-coupled stiffnesses are negligible. However, the non-zero attitude angles observed imply that the cross-coupling coefficients have a definite value. Hence the results are consistent with the steady state journal locus reported herein.

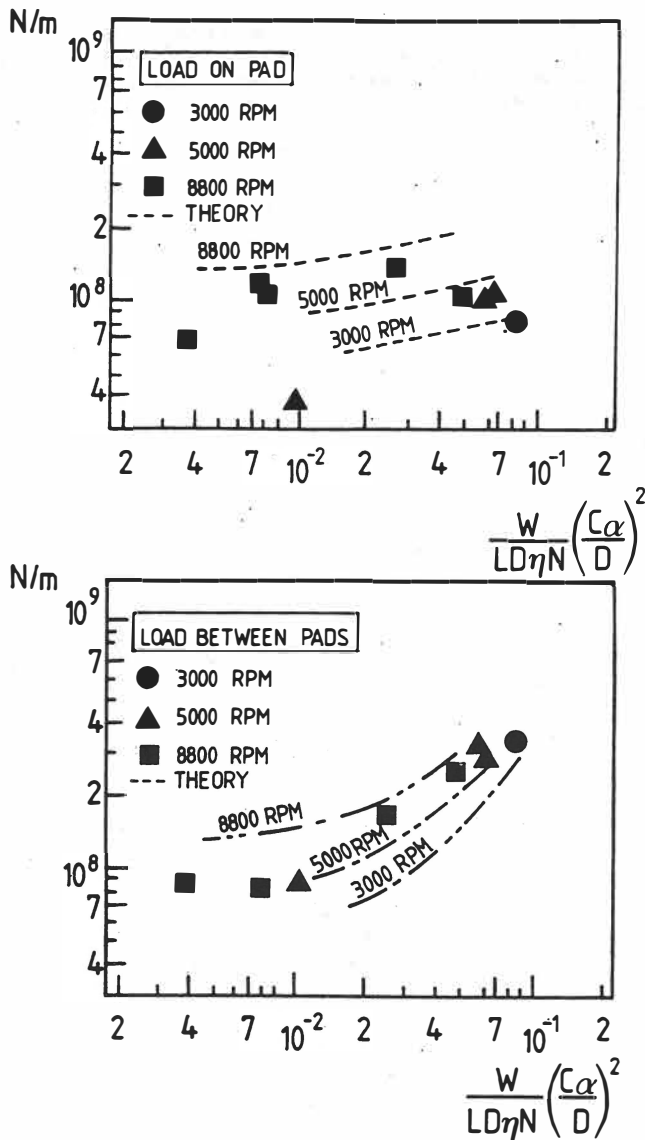


Fig. 8—Measured and predicted stiffness coefficient a_{zz} .

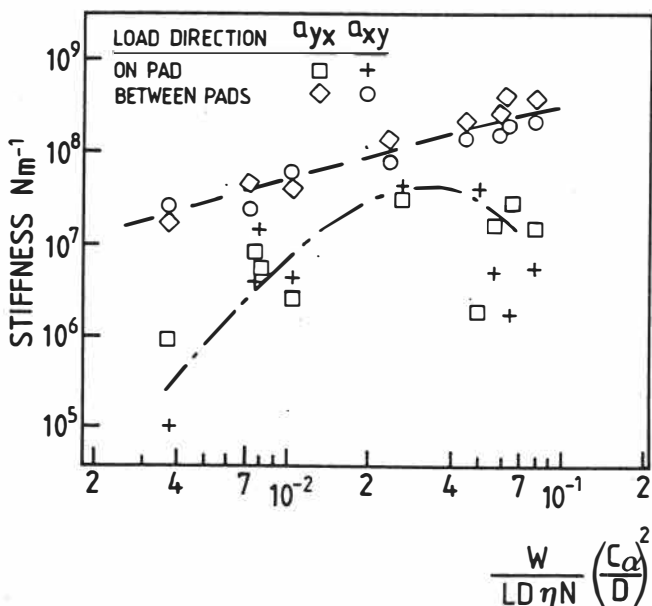


Fig. 9—Measured cross-coupling stiffness coefficients a_{yx} and a_{xy} .

CONCLUDING REMARKS

1. A technique has been developed to obtain a satisfactory measurement of the installed bearing clearance space which overcomes the problems due to the pad tilting action when the stationary journal is pressed onto the bearing pads.
2. The test rig configuration enabled load to be directed to the center of either of two pads, or between the same, at any given duty.
3. Techniques have been developed which enable the bearing center to be located in the hot rotating condition. This was separately invoked for each and every set of steady state measurements at a given load-speed combination. Hence, each measured data point on the steady state journal locus, (ϵ, ϕ) was independently obtained. The consistency in the steady state locus for each of the two loading directions is therefore reassuring.
4. Measurements demonstrate that operating temperature is essentially a function of speed and is insensitive to applied load, which agrees well with the predictions of the bearing performance.
5. Measured direct stiffness values demonstrate the characteristics to be expected from this type of bearing. They are in reasonable agreement with the predicted values.
6. The measured cross-coupling stiffness coefficients are somewhat larger than those normally predicted or assumed for this type of bearing. Values for the load between pad condition at larger eccentricities have similar magnitude to the smaller direct coefficient. However, the results formed a consistent trend and are compatible with the attitude angles observed.

ACKNOWLEDGMENTS

The authors wish to thank the Directors of Michell Bearings for permission to publish this paper, and their colleagues both there and at Cranfield Institute of Technology for their assistance.

REFERENCES

- (1) Ettles, C. M., "The Analysis and Performance of Pivoted Pad Journal Bearings Considering Thermal and Elastic Effects," *ASME Jour. of Lub. Tech.*, **102**, pp 172-181 (1980).
- (2) Knight, J. D. and Barrett, L. E., "Analysis of Tilting Pad Journal Bearings with Heat Transfer Effects," *Trans. ASME. Jour. of Trib.*, **110**, pp 128-133 (1988).
- (3) Nicholas, J. C., Gunter, E. J. and Allaire, P. E., "Stiffness and Damping Coefficients for the Five-Pad Tilting Pad Bearing," *ASLE Trans.*, **22**, 2, pp 113-124 (1979).
- (4) Jones, G. J. and Martin, F. A., "Geometry Effects in Tilting Pad Journal Bearings," *ASLE Trans.* **22**, 3, pp 227-244 (1979).
- (5) Brockwell, K. R. and Dmochowski, W., "Calculation and Measurement of the Steady State Operating Characteristics of Five Shoe Tilting Pad Journal Bearing," *Eurotrib 89 Helsinki* (1989).
- (6) Brockwell, K. R. and Kleinbub, D., "Measurement of the Steady State Operating Characteristics of Five Shoe Tilting Pad Journal Bearing," *STLE 1988 Annual Meeting Preprint 88-AM-3D-3*.
- (7) Huang, T., Wang, Y. and Wen, S., "Investigation of Static and Dynamic Characteristics of Tilting Pad Bearing," *Proc. 13th Leeds-Lyon Symposium on Tribology*, Elsevier, Tribology Series 11, (1987) pp 487-494.

D. W. PARKINS AND D. HORNER

- (8) Tripp, H. and Murphy, B., "Eccentricity Measurements on a Tilting Pad Bearing," *ASLE Trans.*, **28**, pp 217-224 (1984).
- (9) Brockwell, K. R. and Dmochowski, W., "Experimental Determination of the Journal Bearing Oil Film Coefficients by the Method of Selective Vibration Orbits," *ASME 12th Biennial Conf. on Mechanical Vibration and Noise* (1989).
- (10) Parkins, D. W., "Static and Dynamic Characteristics of a Hydrodynamic Journal Bearing," PhD Thesis, Cranfield Institute of Technology (1976).
- (11) Parkins, D. W., "Measured Characteristics of a Journal Bearing Oil Film," *ASME Trans. Jour. Lub. Tech.*, **103**, pp 120-125 (1981).